Abstract for the 31st International Workshop on Water Waves and Floating Bodies, Plymouth, MI, USA, April 3~6, 2016

Eigenvalue Approach for Statistical Analyses of the Second-Order Hydrodynamic Responses

By Dong-Hyun Lim[(1)], Taeyoung Kim[(2)], Yonghwan Kim[(1)*]
[(1)]Department of Naval Architecture and Ocean Engineering, Seoul National University, Seoul, Korea
[(2)]Department of Naval Architecture and Ocean Engineering, Samsung Heavy Industries, Daejeon, Korea
E-mail: **yhwankim@snu.ac.kr*

1. Introduction

When an offshore structure is under a severe sea state, the analysis of nonlinear hydrodynamics is essential. Particularly, the second-order hydrodynamic quantities are very important as the design parameters of the offshore structure. The stochastic behaviors of the second-order quantities are known to deviate from the Gaussian distribution model due to nonlinearities, so that either direct simulations in the time-domain or the characteristic function approach in the frequency-domain has been adopted to estimate the probability distribution of them.

In this study, the stochastic behaviors of the second-order hydrodynamic quantities are investigated using a characteristic function approach which involves the eigenvalue analyses with the Hermitian kernels constructed with quadratic transfer functions. Two different second-order responses are considered in the present analyses: springing responses of TLP tendons and the slow-drift motions of a semi-submergible platform moored in waves. The applicability of the characteristic function approach in predicting extreme values for different second-order quantities are assessed by comparing the results with direct simulations in the time domain.

2. Mathematical Background

Let $Y(t)$ be a nonlinear hydrodynamic response at a certain location to unidirectional random excitation, $X(t)$. Then $Y(t)$ can be represented as a functional power series of $X(t)$, i.e. two-term Volterra series:

$$\begin{aligned} Y(t) &= Y_0 + Y_1(t) + Y_2(t) \\ &= h_0 + \int_0^\infty h_1(t_1)X(t-t_1)dt_1 + \int_0^\infty\int_0^\infty h_2(t_1,t_2)X(t-t_1)X(t-t_2)dt_1dt_2 \\ &= h_0 + \mathrm{Re}\left[\sum_{j=1}^{\infty} A_j H_1(\omega_j)e^{i\omega_j t}\right] + \mathrm{Re}\left[\sum_{j=1}^{\infty}\sum_{k=1}^{\infty} A_jA_kH_2(\omega_j,\omega_k)e^{i(\omega_j+\omega_k)t} + \sum_{j=1}^{\infty}\sum_{k=1}^{\infty} A_jA_k^*H_2(\omega_j,-\omega_k)e^{i(\omega_j-\omega_k)t}\right] \end{aligned} \tag{1}$$

$Y_n(t)$ indicates the nth order component of total response $Y(t)$, and $h_1(t_1)$ and $h_2(t_1, t_2)$ are linear and quadratic impulse response functions respectively. We hereby neglect the zero-th order term Y_0 since it is not a stochastic variable. This is the case when the random excitation $X(t)$ be expressed as a sum of sinusoidal component waves, i.e. $X(t) = \mathrm{Re}\left[\sum_{j=1}^{\infty} A_j e^{i\omega_j t}\right]$. In the equations above, ω_j and A_j indicate the frequency and the complex amplitude of jth wave component respectively, and $H_1(\omega_j)$ and $H_2(\omega_j, \omega_k)$ represent the linear transfer function (LTF) and the quadratic transfer function (QTF) respectively. Upper script $(\,)^*$ indicates the complex conjugate of a quantity.

Let $X(t)$ be expressed as an equivalent filtered white noise process with weighting function $a(\tau)$ and a unit white noise $N(t)$ as follows.

$$X(t) = \int_{-\infty}^{\infty} a(\tau)N(t-\tau)d\tau \tag{2}$$

Expanding $N(t\text{-}\tau)$ with basis functions $\phi_j(t)$ and standardized Gaussian variates $X_j(t)$ as in equation (3), the first- and second-order responses are expressed as equations (4) and (5).

$$N(t-\tau) = \sum_{j=1}^{\infty} X_j(t)\phi_j(\tau) \tag{3}$$

$$Y_1(t) = \sum_{j=1}^{\infty} C_j X_j(t),\ \ C_j = \int_{-\infty}^{\infty}\int_{-\infty}^{\infty} h_1(\tau)a(\alpha)\phi_j(\tau+\alpha)d\alpha d\tau \tag{4}$$

$$Y_2(t) = \sum_{j=1}^{\infty}\sum_{k=1}^{\infty} X_j(t)X_k(t)\int_{-\infty}^{\infty}\int_{-\infty}^{\infty} \phi_j(\alpha)\phi_k(\beta)K(\alpha,\beta)d\alpha d\beta \tag{5}$$

where

$$K(\alpha,\beta) = \int_{-\infty}^{\infty}\int_{-\infty}^{\infty} a(\alpha-\tau_1)a(\beta-\tau_2)h_2(\tau_1,\tau_2)d\tau_1 d\tau_2 \tag{6}$$

Then, the basis functions $\phi_j(t)$ are required to be the eigen functions of the integral equation (7),

$$\int_{-\infty}^{\infty} K(\alpha,\beta)\phi_j(\beta)d\beta = \lambda_j\phi_j(\alpha) \tag{7}$$

Since the kernel $K(\alpha, \beta)$ of the integral equation is symmetric the eigen functions $\phi_j(t)$ are orthonormal, the expression

for $Y_2(t)$ in equation (5) can be simplified as follows:

$$Y_2(t) = \sum_{j=1}^{\infty} \lambda_j \left[X_j(t) \right]^2 \tag{8}$$

The characteristic function of a random variable is defined as the inverse Fourier transform of the probability density function. Then the characteristic function of the total response $Y(t)$ becomes:

$$F_Y(\theta) = \int_{-\infty}^{\infty} p_Y(Y) e^{i\theta Y} dY = E e^{i\theta\left(\sum_{j=1}^{\infty} C_j X_j + \sum_{j=1}^{\infty} \lambda_j X_j^2\right)} = \prod_{j=1}^{\infty} E\left[e^{i\theta\left(C_j X_j + \lambda_j X_j^2\right)} \right] \tag{9}$$

Since X_j are a standardized Gaussian variate, $F_Y(\theta)$ is analytically expressed as below:

$$F_Y(\theta) = \prod_{j=1}^{\infty} \int_{-\infty}^{\infty} \frac{1}{\sqrt{2\pi}} e^{-\frac{1}{2}X_j^2} \cdot \left[e^{it\left(C_j X_j + \lambda_j X_j^2\right)} \right] dX_j = \frac{1}{\prod_{j=1}^{\infty} \left(1 - 2i\lambda_j t\right)^{1/2}} e^{-\sum_{j=1}^{\infty} \frac{C_j^2 t^2}{2(1-2i\lambda_j t)}} \tag{10}$$

and the probability distribution of the response $Y(t)$ is computed by Fourier transforming the characteristic function.

$$p_Y(Y) = \frac{1}{2\pi} \int_{-\infty}^{\infty} F_Y(\theta) e^{-iY\theta} dt \tag{11}$$

For the second-order component $Y_2(t)$, we can simply put C_j=0. Therefore, if the eigenvalue problem in equation (6) can be solved, the probability density function is obtained explicitly.

Since QTF in the frequency domain is normally solved, the kernel $K(\alpha, \beta)$ is desired to be transformed into a frequency-domain expression. This is done by defining new eigenfunctions $\psi_j(\omega)$ as follows (Neal, 1974):

$$\psi_j(\omega) = \frac{1}{2\pi} \sqrt{S_X(\omega)} \int_{-\infty}^{\infty} \int_{-\infty}^{\infty} e^{-i\omega t} a(u-\tau) \phi_j(u) du d\omega \tag{12}$$

where $S_X(\omega)$ is the energy spectrum of the input wave $X(t)$. Then, the eigenvalue problem is expressed in the frequency domain as below with a newly defined Hermitian kernel $K(\omega_1, \omega_2)$:

$$\int_{-\infty}^{\infty} K(\omega_1, \omega_2) \psi_j(\omega_2) d\omega_2 = \lambda_j \psi_j(\omega_1) \tag{13}$$

$$K(\omega_1, \omega_2) = \sqrt{S_X(\omega_1)} H_2\left(\omega_1, -\omega_2\right) \sqrt{S_X(\omega_2)} \tag{14}$$

In the design point of view, the estimation of the exceedance probability of peaks is an essential task. However, the probability of $Y_2(t)$ is not enough for this task and the joint probability density functions of Y, $\dot{Y}$ and $\ddot{Y}$ should be obtained. This is not an easy task. However, if the response spectra are narrow-banded, the derivation of the peak distribution can be drastically simplified.

Let the probability of peaks lying in the range a to $a+da$ be denoted by $p_p(a)da$. In the case of narrow-banded process, the average number of cycles of zero up-crossing is identical to that of the total positive peaks (Kim, 2008), hence the probability which exceeds a can be expressed as

$$\Pr\{\text{peak value} > a\} = \int_a^{\infty} p_p(a) da = \frac{f_a^+}{f_0^+} \tag{15}$$

where f_a^+ represents the averaged crossing frequency of positive slope at $Y = a$. According Newland (1984), f_a^+ is given as

$$f_a^+ = \int_0^{\infty} p_{Y\dot{Y}}(a, \dot{Y}) \dot{Y} d\dot{Y} \tag{16}$$

where $p_{Y\dot{Y}}$ is the joint probability density function between Y and $\dot{Y}$. However, since a random process and its first time derivative are statistically independent (Kim, 2008), the joint probability density function becomes the product of each of the probability density functions. Then, equation (15) can be transformed as

$$\Pr\{\text{peak value} > a\} = \frac{\int_0^{\infty} p_Y(a) p_{\dot{Y}}(\dot{Y}) \dot{Y} d\dot{Y}}{\int_0^{\infty} p_Y(0) p_{\dot{Y}}(\dot{Y}) \dot{Y} d\dot{Y}} = \frac{p_Y(a) \int_0^{\infty} p_{\dot{Y}}(\dot{Y}) \dot{Y} d\dot{Y}}{p_Y(0) \int_0^{\infty} p_{\dot{Y}}(\dot{Y}) \dot{Y} d\dot{Y}} = \frac{p_Y(a)}{p_Y(0)} \tag{17}$$

where $p_{\dot{Y}}$ is a probability density function of $\dot{Y}$. Hence the exceedance probability distribution of peaks of the response can be calculated without any requirement of $p_{Y\dot{Y}}$ under the assumption of small band-width.

3. Applications

3.1 Sum-Frequency Springing on TLP

To validate the present method, the extreme springing tension on a TLP model with 4 tendons is considered (Kim and Yue, 1991; Eatock Taylor and Kernot, 1999). The principal particulars and configurations are presented in Table 1 and Fig. 1. Total pretension is about a quarter of total displacement. It is assumed that the tension is linear.

The sum-frequency QTFs of tensions are obtained by using the results of WADAM and an irregular wave signal is generated from the Bretschneider spectrum with 7-meter significant wave height (Hs), 15-second modal period (Tp), and uniformly distributed random phase. Then the sum-frequency tension signals are generated by the combinations of irregular wave and QTFs of tension, as in Fig. 2(a) and the probability density function of the sum-frequency tension are presented in Fig. 2(b). For the validation of the eigenvalue approach, probability is also measured from the results of direct simulation in Fig. 2(a). Both results are almost the same to each other.

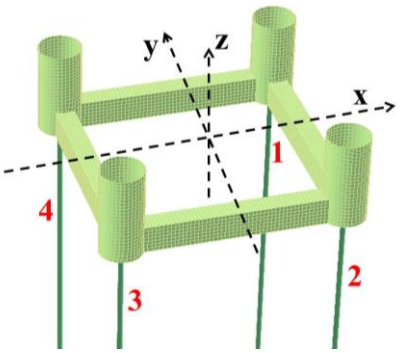

Fig. 1 Configuration of TLP and tendon numbers

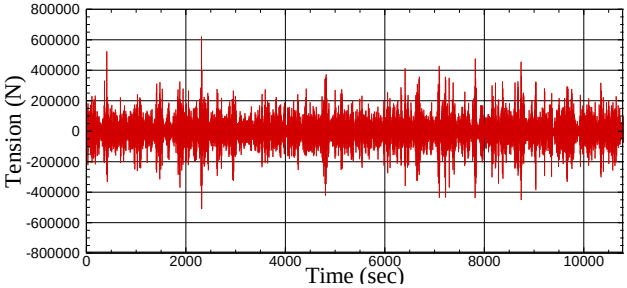

(b) Tension in tendons 1 and 2

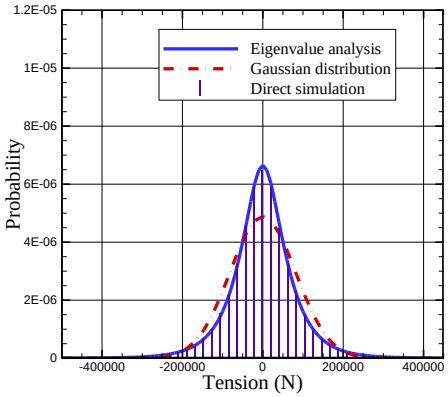

(c) Tension in tendons 3 and 4

Fig. 2 Time history and PDF of the induced sum-frequency tension: Hs=7m, Tp=15sec, head sea

Fig. 3 shows the expected maximum tension by springing. The results of direct simulation are also plotted by selecting and arranging the peak from time-histories in Fig. 2(a). The present method shows reasonable agreement with the direct simulation. The responses by Rayleigh distribution is presented together to compare the difference with linear analysis. Rayleigh distribution definitely underestimates the maximum tension. The difference becomes larger as design life cycle becomes longer.

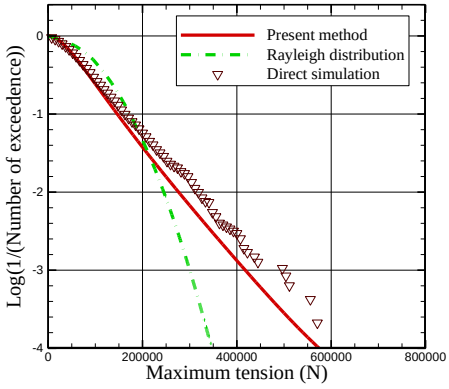

(a) Tendons 1 and 2

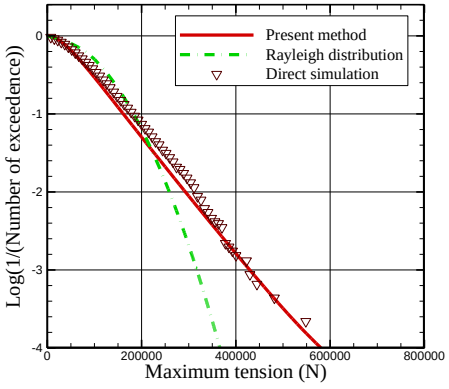

(b) Tendons 3 and 4

Fig. 3 Extreme value prediction of sum-frequency tension force (Hs=7m, Tp=15sec, 3 hours simulation for direct computation)

3.2 Slowly-Varying Motion of Semi-Submergible Platform

For the difference-frequency case, the slowly-varying motion of a semi-submergible platform is considered for the comparison with direct simulation and the present eigenvalue approach. Fig.4 and Table 1 show the test model and its characteristic quantities. In the case of direct simulation, The SML (SWIM-MOTION-LINES) is used, which is capable of the linear and the second-order hydrodynamic analyses in the frequency domain, and the platform/mooring lines coupled analysis in the time domain (Emmerhoff, 1994; Kim & Sclavounos, 2001).

Fig. 5 shows the probability density function and the probability of exceedance for peak values of surge motion when the motion and mooring lines are not coupled. Like the sum-frequency case shown above, the present approach

provides an excellent agreement with direct simulation. However, it is found that the body motion and mooring are coupled, it is found that the probability density of surge motion is can be well predicted using Rayleigh distribution. The details will be presented in the workshop.

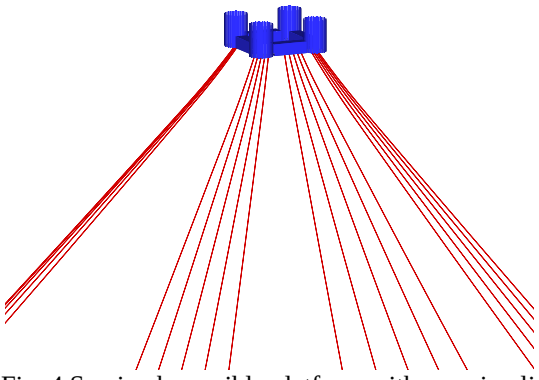

Fig. 4 Semi-submergible platform with mooring lines

Pontoon length	43.5 (m)
Pontoon breadth	15.0 (m)
Pontoon depth	14.5 (m)
Cylinder diameter	29.0 (m)
Draft	40.0 (m)
Displacement	143,528 (ton)
KG	33.0 (m)
Water depth	3,048 (m)
Pre-tension	1,258 (kN)
Number of lines	20
Angle between the lines in one group	5 (°)
Total length of one mooring line	4267.14 (m)

Table 1 Characteristics of semi-submergible platforms

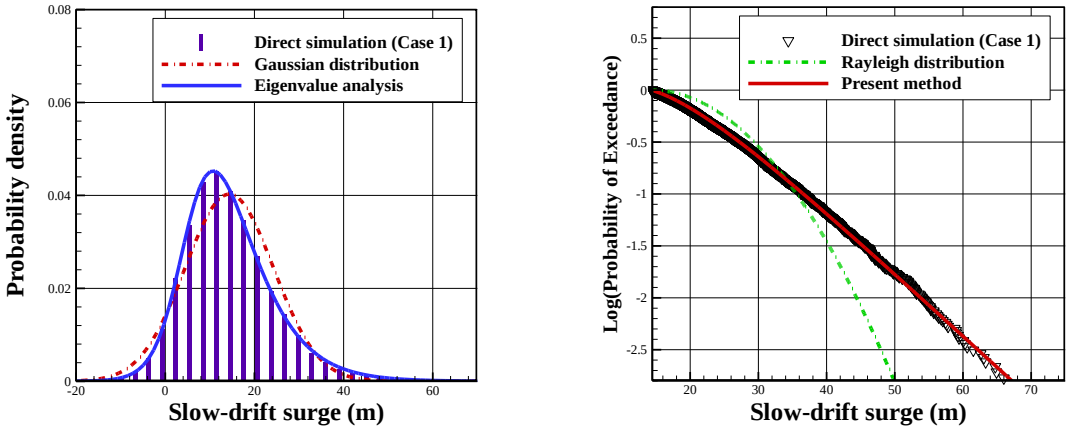

(a) PDF (b) Probability of exceedance

Fig. 5 Probability density function and the probability of exceedance for peaks of surge motion: without coupling

Acknowledgement

This study is supported by the Global Leading Technology Program of the Office of Strategic R&D Planning(OSP) funded by the Ministry of Trade, Industry and Energy, Republic of Korea (Project No: 10042556), and Hyundai Heavy Industries. Their supports are greatly appreciated.

References

Eatock Taylor, R., and Kernot, M.P., 1999, On second order wave loading and response in irregular seas, Advances in Coastal and Ocean Engineering, 5, World Scientific, Singapore.

Emmerhoff, O.J. (1994). *The Slow-Drift Motions of Offshore Structures*, Ph.D. Thesis, MIT.

Kim, C.H., Zhao, C., and Zou, J., 1995, Springing and ringing due to nonlinear waves on a coupled TLP, Proceedings International Offshore and Polar Engineering Conference, Hague, Netherlands, 83-89.

Kim, M.H., and Yue D.K.P., 1991, Sum- and difference -frequency wave loads on a body in unidirectional Gaussian seas, Journal of Ship Research; 35 (2), 127-140.

Kim, S. and Sclavonous, P.D. (2001). "Fully Coupled Response Simulations of Theme Offshore Structures in Water Depths of Up to 10,000 Feet", *Proceedings of the Eleventh(2001) International Offshore and Polar Engineering Conference(ISOPE)*, Vol.3, 457-466.

Naess, A., and Ness, G.M., 1992, Second-order sum-frequency response statistics of tethered platforms in random waves, Applied Ocean Research; 14 (1), 23-32.

Naess, A., 1994, Statistics of combined linear and quadratic springing response of a TLP in random waves, Journal of Offshore Mechanics and Arctic Engineering; 116 (3), 127-136.